AF2008114

Analysis of Current Sectors Based on Traffic and Geometry

Gano B. Chatterji* and Yun Zheng†
University of California Santa Cruz, Moffett Field, CA, 94035-1000
and
Parimal Kopardekar‡
NASA Ames Research Center, Moffett Field, CA, 94035-1000

This paper describes an evaluation of current sectors in the continental United States using a variety of traffic and geometric metrics. Most of the metrics have been computed using real track-data. In instances where this was not possible, simulated traffic data are used. Statistics of these metrics are summarized for higher altitude sectors in the twenty air route traffic control centers and in eight geographical regions. The analysis shows that most sectors have fewer than twenty aircraft and three conflicts at any given time. Air traffic in higher altitude sectors consists of mostly jets that fly in a narrow range of airspeeds and altitudes. A wide variation was found in the volume, area, height, length and transit times of the sectors. Most sectors were found to be elongated and aligned in the direction of the traffic flows. The properties of today's sectors reflect the technologies and procedures used for air traffic control. With the introduction of automation, the design of airspace partitions will not be contrained by how controllers manage traffic. However, if controllers are involved to some degree in the future system, it might be useful to account for some of the characteristics of the current sectors in the design of future airspace partitions.

I. Introduction

In the current national airspace system, design of sectors have evolved over a long period of time based on incremental addition of new technologies and procedures for air traffic control. Each sector has a fixed capacity. When these capacities are exceeded by traffic demand, traffic flows are restriced to bring the demand below capacity. The concept in Ref. 1 suggests that instead of restricting traffic, which causes delays, airspace capacity can be increased by partitioning the airspace differently. Motivated by this concept, several methods for airspace partitioning that are described in Refs. 2 through 6 have been developed. These methods use some measure of controller workload to guide the design. In the future, with increased level of automation, airspace design might not be guided by controller workload considerations. Depending on how different the future design is from the current design, the controller's ability to actively separate aircraft might be limited. It might be useful to carry some of the design features of the current system into the future one, if some role for human controller is envisioned in the future air traffic control system. The motivation for computing metrics for the existing sectors is to capture some of the design features of the current sectors.

Since the design of current sectors is based on the routes of flight and controller workload considerations, metrics related to controller workload can be expected to capure the design features. There are numerous traffic and geometry metrics described in the literature that have been found to be useful for modeling controller's perception of workload and in operational error studies.[7-11] These studies are limited to sectors in few centers. A comprehensive study of sectors in all the twenty centers is unavailable.

In this paper, thirty-three traffic and geometric metrics from Refs. 7 to 11 are computed for 364 higher altitude sectors in each of the twenty centers, and in eight geographical regions. Higher altitude sectors were chosen because the benefits of airspace partitioning are expected to be realized in these sectors first. Data presented in this paper describes the design of the current sectors and will be found to be useful for comparing the designs of future airspace partitions.

---

* Principal Scientist and Task Manager, U. C. Santa Cruz, MS 210-8, Associate Fellow.
† Software Engineer, U. C. Santa Cruz, MS 210-8.
‡ Associate Principal Investigator, Automation Concepts Branch, MS 210-10, Senior Member.

The paper is organized as follows. Section II describes the method for computing the metrics for each sector. The maximum number of aircraft in sectors obtained using simulated track-data are compared with those obtained using actual track-data in this section. Evaluation of sectors based on the traffic metrics is described in Section III and on geometric metrics in Section IV. Finally, the paper is summarized in Section V.

II. Computational Method

This section describes two methods for computing the fifteen sector traffic metrics as a function of time. The first method processes the actual track-data, and the second method processes simulated traffic data. The main benefit of using actual track-data is that they best represent traffic resulting from the demand and capacity constraints of the particular day. These data reflect flow control and separation assurance actions, and airline operational control actions such as: cancellations and creation of new flights. Along with their benefits, they suffer from some data-quality issues discussed in Ref. 12 that can lead to erroneous values of the metrics.

Simulated traffic data do not suffer from many of the data quality issues, but they do not include all of the real-world effects. Trajectories of aircraft are simulated using mathematical models; they can be expected to differ from those actually flown. Simulated traffic data have to be compared against actual traffic data for validation. These limitations not withstanding, a simulation offers far greater flexibility in designing scenarios, including future traffic growth scenarios, for evaluating the desired metrics. Simulation also provides a mechanism for eliminating control actions inherent in the real system. For example, aircraft are permitted to violate separation minimums, which only happen as an operational error in the real system. Given a choice between using actual position data, "track-data," and simulated data, it is often desirable to use the actual track-data because they represent reality. Due to this reason, ten of the fifteen measures have been computed using the actual track-data derived from a recorded Airline Situation Display to Industry (ASDI) file. The remaining five metrics, number of jet aircraft, number of non-jet aircraft, conflict-count, average airspeed and variance in airspeed, were computed using position data simulated using the Airspace Concept Evaluation System (ACES) with flight-plans extracted from the same ASDI file. The reason for using simulated data is that the information needed for computing these metrics is provided in the flight plan and not in the actual track-data.

A. Track-Data

The ASDI subsystem of the Enhanced Traffic Management System (ETMS)[13] disseminates real-time air traffic data, associated with different message types, to aviation industry. Of the different ASDI messages and supported data types described in Ref. 13, only the track/flight data-block messages, TZ messages, were used for computing the traffic metrics. TZ messages contain time-stamp, ARTCC identifier, aircraft identification (ACID), groundspeed, altitude, latitude and longitude. Over 9 million TZ messages were extracted from the recorded ASDI file, containing 48-hours of traffic data spanning the period from zero Coordinated Universal Time (UTC) on 17 March 2006 to zero UTC on 19 March 2006. Traffic data for these days were selected because of high traffic-volume, low weather impact and low delays. It should be noted that the traffic patterns vary from day to day and from season to season depending on demand, capacity, wind patterns and weather. Numerical values of the metrics in the sectors can be expected to vary based on the traffic pattern. The results presented in this paper are for a nominal day, which is defined as a high-volume, low-weather, and low-delay day.

The time-sorted TZ messages were stored in data structures based on ACID. Data structures were then examined for each ACID to determine all the flights associated with that ACID. Individual flights were identified based on temporal gaps in the associated time-stamps. A temporal spacing of over thirty minutes was assumed to be due to a different flight. After identifying each flight, duplicate messages within one-minute periods were removed. This reduced the data by about 15%.

Each flight's latitude, longitude and altitude derived from TZ messages were used to determine the sector the flight was in at each instant of time, where the sectors were as defined in May 2007 ETMS adaptation data. An efficient procedure for locating aircraft in a sector, described in Ref. 14, was used to identify the sectors. The latitudes and longitudes were then transformed into Cartesian coordinates with respect to a horizontal frame of reference using Oblique Stereographic Projection.[2] A first-order filter with altitude time-history input was used to generate time-history of climb/descent rate of each flight. Time, Flight ID, climb/descent rate, position and the sector corresponding to the position were input into a *MySQL*[15] database. This database was then queried to extract data related to flights in each sector and to sort them in time. These time-sorted data were then used to determine the numbers of aircraft in climb, in cruise, and in descent, and their sum (total number of aircraft) in the sectors.

The data and the results are for 364 higher altitude sectors shown in Fig. 1. Each of these sectors has a floor of 17,100 feet altitude or higher. Fifty of the sectors have a floor between 17,100 feet and 24,000 feet; the rest have a

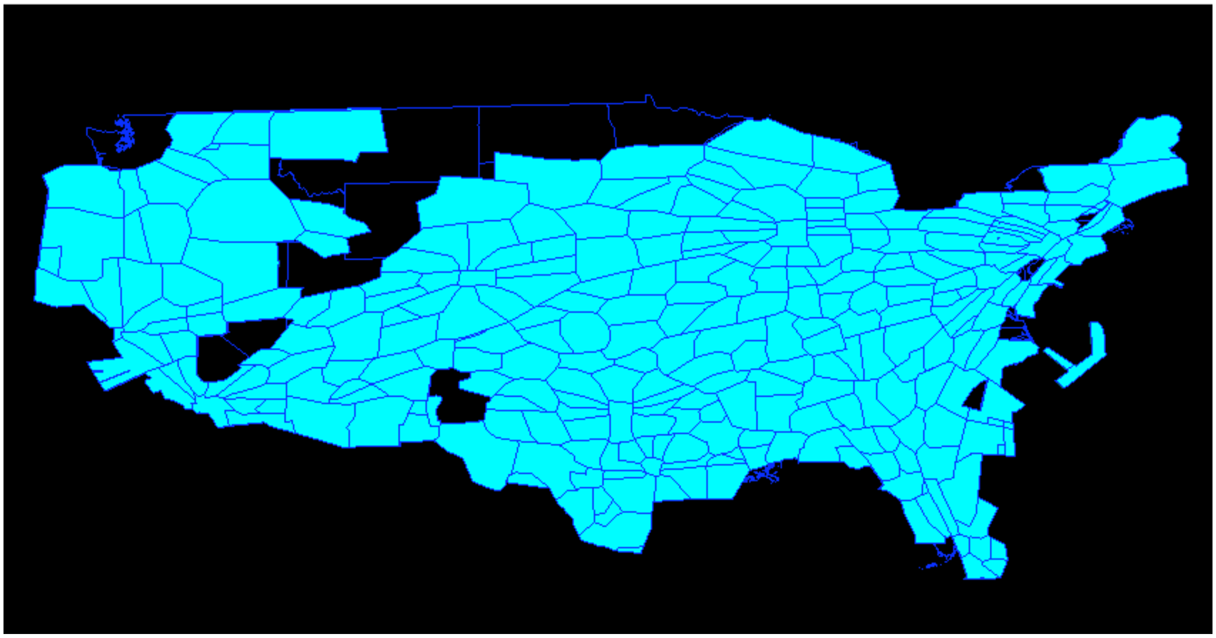

Figure 1. View of 364 higher altitude sectors with a floor at or above 17,100 feet altitude.

floor at or above 24,000 feet altitude. The ceilings of these sectors are between 24,000 feet and 99,900 feet altitude. Several sectors in Salt Lake, Minneapolis, New York, DC, Boston and Los Angeles centers (see Fig. 1) were not included in the analysis because their floors are below 17,100 feet altitude.

B. ACES Simulation

ACES is a comprehensive computational model of the national airspace system consisting of air traffic control and traffic flow management models of ARTCCs, terminal-radar-approach-controls (TRACON), airports and the air-traffic-control-system-command-center (ATCSCC).[16] It simulates flight trajectories through the enroute-phase of flight, where enroute-phase for jet aircraft is above 10,000 feet. A queuing model simulates surface movement and flight through terminal airspace. Traffic flow management and air traffic control models in ACES use airport and sector capacity thresholds for delaying flights, while they are on the ground and during their enroute-phase. Some of the ACES outputs are arrival and departure counts at airports, traffic-counts in sectors and air traffic system performance metrics including arrival, departure, enroute and total delays. Earlier validation studies in Refs. 17 and 18 have shown that ACES generates realistic delays and airport operational metrics similar to those observed in the real-world. Due to these capabilities, ACES was chosen for simulating traffic.

Table 1. Sector capacities.

MAP	No. of sectors
9	1
10	1
11	5
12	10
13	15
14	23
15	62
16	45
17	28
18	82
19	38
20	22
21	31
23	1

Simulation Inputs

ACES simulation inputs include files containing capacity data (airport arrival and departure capacities, and sector capacities), traffic data (scheduled departure times and flight-plans), and adaptation data (sector/center geometric data).

The actual airport arrival and departure rates specified at the 74 major U. S. airports on 17th and 18th March 2006 were specified as airport capacities in ACES. Sector capacity data were derived from the ETMS data tables. Sector capacity is defined as the maximum number of aircraft allowed in a sector at any one time during a fifteen-minute time interval. Capacity values, known as Monitor Alert Parameter (MAP), are used in the ETMS to trigger traffic flow management initiatives for demand reduction. Capacity thresholds are set to ensure that air traffic controllers are able to separate aircraft traversing the sector airspace. MAP values and the number of sectors with those values out of 364 higher altitude sectors are shown in Table 1. The average MAP value is approximately 17 and the most frequent MAP value is 18 for data in Table 1.

Flight-plans for the simulation were derived from the same ASDI file used for computing the traffic-count metrics discussed in the previous subsection. Flight connectivity data relating the same physical aircraft to two or more flights segments were obtained from the Bureau of Transportation Statistics (BTS) for the two days. Airline flight-numbers, aircraft tail-numbers and the associated flight-plans for all flights were included in the ACES input file. Scheduled departure times derived from the BTS data were assigned as departure times. Proposed departure times from flight-plan messages in the ASDI data, or actual departure times in ASDI data minus average taxi times associated with airports of departure were assigned as departure times when scheduled times were not available in the BTS data.

After assigning scheduled departure times for flights, an ACES simulation was run without airport and sector capacity constraints to compute unconstrained arrival times of flights at their destination airports. These were then set to scheduled arrival times at destination airports. A series of steps described in Ref. 19 were then taken to ensure that flight connectivity was preserved and that the arrival and departure schedules were compatible with turn-around-time requirements, time required for unloading aircraft after arrival at the gate and preparing it for departure. Final traffic schedule was generated after making the required flight schedules and tail-number changes.

Sector and center geometry definitions needed for the simulation were obtained from the May 2007 ETMS adaptation data.

Simulation Outputs

ACES writes out identification information (ID) and position coordinates of flights that are in each sector to an output database at the specified rate during simulation. After completion of the simulation, flight IDs associated with a sector and their position time-histories were extracted from the database for computation of the five traffic metrics, number of jet aircraft, number of non-jet aircraft, conflict-count, average airspeed and variance in airspeed. This process was repeated for every sector.

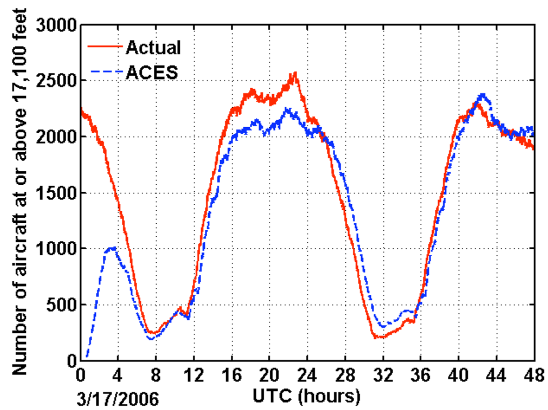

Figure 2. Actual and ACES simulated aircraft-counts.

C. Comparison of Tack-Data and ACES Simulation Results

Given that there are differences between the actual traffic data from the field and ACES simulated data, it is necessary that a comparison between the values of metrics obtained by processing actual track-data and ACES simulation be done for establishing the validity of the results. This was accomplished by comparing 1) the total number of aircraft in higher altitude airspace and 2) numbers of higher altitude sectors grouped according to the peak total-counts (traffic-counts), peak climb-counts, peak cruise-counts and peak descent-counts in each hour simulated by ACES with those obtained by processing track messages.

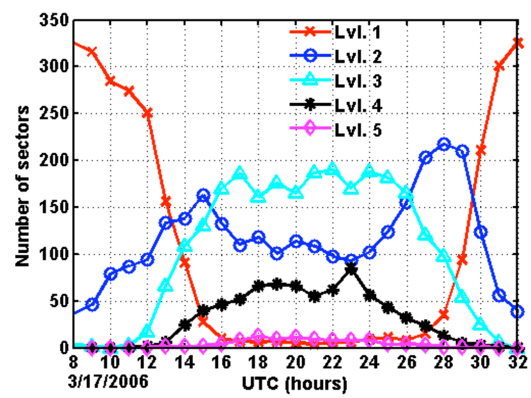

Figure 3. Sectors with peak traffic-count in the first five levels, listed in Table 2, using actual track-data.

Numbers of aircraft in sectors shown in Fig. 1 were retrieved from the simulation output and added together to compute the total number of aircraft in ten-second intervals. This time-history is shown with that of the actual number of flights in Fig. 2. Observe that the ACES simulation starts with all aircraft on the ground, whereas in the actual air traffic system there are always flights that are airborne. Figure 2 shows that the simulated traffic catches up with the actual traffic. The general trends of simulated and actual traffic are similar for the twenty-four hours between eight UTC on 17 March 2006 and eight UTC on 18 March 2006 (location marked 32 UTC in Fig. 2). Some of the differences between the time-histories are attributable to the issues with simulated and actual flight data discussed earlier in this section.

For comparison based on peak traffic-counts, aircraft were counted in each higher altitude sector. The maximum of 60 values, one for each minute, provided the maximum number of aircraft, peak traffic-count, using actual track data for that hour. Figures 3 and 4 show the number of sectors with peak traffic-count values in the first five levels listed in Table 2 during each one-hour period. The graphs in the figures viewed in conjunction with Fig. 2 show that as traffic increases, there are fewer sectors with low peak traffic-counts as would be expected. The maximum numbers of sectors for the four graphs, Level 2 through 5, in Fig. 3 were found to be 217 at 28:00 UTC, 190 at 22:00 UTC, 85 at 23:00 UTC and 12 at 18:00 UTC. In Fig. 4 these are 222 at 29:00 UTC, 176 at 24:00 UTC, 55 at 23:00 UTC and 12 at 17:00 UTC.

Table 2. Peak traffic-count levels.

Level	Peak Traffic-Count Range
1	0 - 4
2	5 - 9
3	10 - 14
4	15 - 19
5	20 - 24
6	25 – 29
7	30 - 34
8	> 34

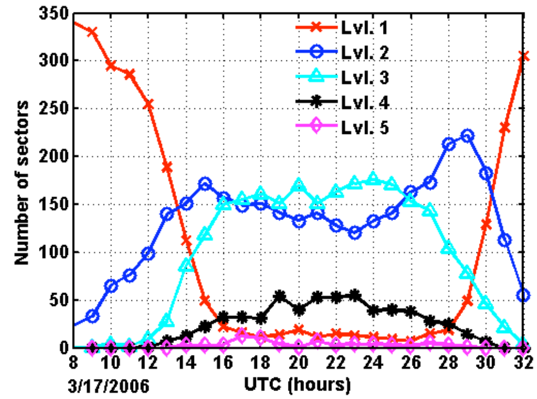

Figure 4. Sectors with peak traffic-count in the first five levels, listed in Table 2, using ACES data.

The information contained in the individual graphs in Figs. 3 and 4 can be combined and presented in terms of a vertically stacked bar chart for each one-hour period of the day. Such bar charts provide cumulative information as explained by the following example. Consider the bar charts obtained by processing the actual track-data shown in Fig. 5. Of the eight levels listed in Table 2 and included in Fig. 5, only levels one through five are visible in the bar charts. Numbers of sectors with a peak traffic-count of four aircraft or less are shown in the bottom bar charts. Numbers of sectors with the next higher level are placed on top of this layer, and so on.

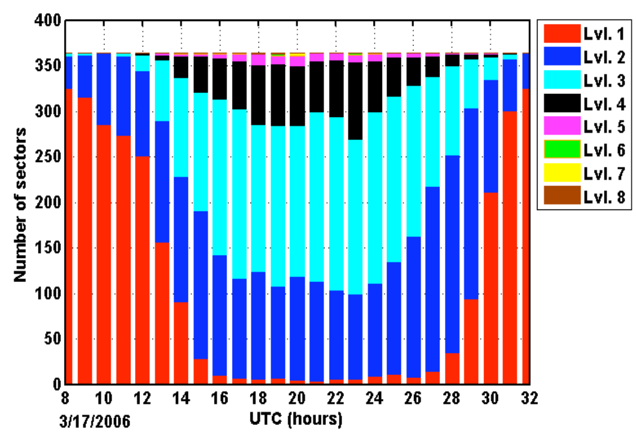

Figure 5. Time-history of bar charts of number of sectors grouped in eight peak traffic-count levels using track-data.

Cumulative counts obtained by summing the levels below each chosen level determine the numbers of sectors with peak traffic-counts below the thresholds implicitly defined by levels in Table 2. For example, the top of Level 2 histogram at 23:00 UTC indicates that at any time of the day, at least 99 sectors have a peak traffic-count of nine aircraft or less. This is defined as the lower cumulative count. The maximum value of the top of the Level 2 histogram is 364 sectors at 10:00 UTC. This maximum value is defined as upper cumulative count. Table 3 summarizes these results obtained using actual track-data and ACES simulation.

Table 3. Numbers of sectors with peak traffic-counts below thresholds using ACES simulation compared to those obtained using track-data.

Threshold	Track-Data	ACES Simulation
5	4	7
10	99	133
15	269	303
20	350	352
25	361	362
30	362	364
35	363	364
42	364	364

The time-histories shown in Figs. 3 and 4 compare reasonably well; they show that similar peak traffic-counts are obtained in approximately the same number of higher altitude sectors using actual track-data and ACES simulated track-data. Values listed in the second and third columns of Table 3 also suggest that the peak traffic-count statistics computed using actual track-data and ACES are comparable. Analysis of peak climb-counts, peak cruise-counts and peak descent-counts using actual track-data and ACES simulated data also compared well.

III. Traffic Metrics

A considerable amount of research has been devoted to the synthesis of traffic dependent metrics and their application to modeling sector complexity and air traffic controller's workload.[8,9] Traffic metrics that were found to be especially pertinent for modeling workload perceived by controller in Ref. 8 are listed in Table 4. These metrics were computed for today's higher altitude sectors shown in Fig. 1 and the results are presented in the following subsections.

Table 4. Traffic metrics.

Number	Metric	Data	Type
1	Maximum number of aircraft	Actual	Count
2	Maximum number of aircraft in climb	Actual	Count
3	Maximum number of aircraft in cruise	Actual	Count
4	Maximum number of aircraft in descent	Actual	Count
5	Maximum number of jet aircraft	Simulated	Count
6	Maximum number of non-jet aircraft	Simulated	Count
7	Peak conflict-count	Simulated	Count
8	Average horizontal separation between aircraft in sector	Actual	Separation
9	Minimum horizontal separation between aircraft in sector	Actual	Separation
10	Average vertical separation between aircraft in sector	Actual	Separation
11	Minimum vertical separation between aircraft in sector	Actual	Separation
12	Average time-to-go to conflict	Actual	Separation
13	Sector average transit time	Actual	Flow
14	Average airspeed	Simulated	Flow
15	Variance in airspeed of aircraft	Simulated	Flow

A. Traffic-count Metrics

Peak traffic-count or the maximum number of aircraft has been found to be the most important contributor to controller workload. Research has found that controller activity and attentiveness are highly correlated to peak traffic-count.[10] Maximum number of aircraft in higher altitude sectors computed using actual track-data were discussed in Section II. The time histories of the numbers of sectors with peak traffic-count levels were shown in Fig. 3 and the corresponding bar charts were shown in Fig. 5.

Maximum numbers of aircraft in the climb phase (peak climb-count), in the cruise phase (peak cruise-count), and in the descent phase (peak descent-count) were computed in the same manner as the peak traffic-count in a sector. Aircraft with a climb rate of 200 feet/minute or more were considered to be climbing and those with a descent rate greater than or equal to 200 feet/minute were considered to be descending. Aircraft with climb or descent rates less than 200 feet/minute were considered to be cruising.

Maximum number of jet aircraft and non-jet aircraft (turboprops and piston-props) in each hour in every sector were computed using ACES simulated track-data at ten second intervals. Since actual track-data do not contain aircraft type information, flight plans do, ACES simulated track-data that are based on flight-plans were used. Although it is possible to relate actual track-data to the flight-plans using the aircraft IDs that are common to both the message types, it does require an efficient data structure, significant memory and computation.

ACES simulated data were also used for computing conflict-counts. Since jet aircraft cruise at approximately 8 miles/minute, trajectory data generated by ACES were written to the output database at ten-second intervals. Aircraft within each sector were selected from the database for checking conflicts, which means that conflicts between aircraft in neighboring sectors were not checked. This limitation arose because the database did not contain information on which sector is next to which one. Not knowing the sector neighborhood relationship meant that the only way to check for all such conflicts was to consider all the flights at each time-

Table 5. Numbers of sectors with peak climb-counts using actual track-data.

Level	Min.	Mean	Max.	Threshold	Cumulative Lower	Cumulative Upper
1	282	323	363	5	282	363
2	1	40	80	10	359	364
3	0	1	5	15	364	364

instant, which is a compute intensive process. Two aircraft were considered to be in conflict if the vertical separation was less than 1,000 feet and the horizontal separation was five nautical-miles or less.

Time histories of numbers of sectors at the eight levels of Table 2 (such as in Figs. 3, 4 and 5) were generated for each of the traffic-count metrics discussed above. These were then processed further to compute minimum, mean, maximum and cumulative counts. The computed values are provided in Tables 5 through 10. Table 5 lists the values for maximum number of aircraft in climb. The first column indicates levels from Table 2. The second column lists the minimum number of sectors at the indicated level at any given time. For example, the minimum value of 282 for Level 1 means that at least 282 sectors have between zero and four aircraft climbing at any given time. The value of 323 in the third column indicates that on an average, 323 sectors have four or fewer aircraft in climb phase. Similarly, the maximum value of 363 in the fourth column indicates that at most 363 sectors have four or fewer climbing aircraft during the 8:00 UTC to 32:00 UTC time range. The fifth column lists the maximum climb-count thresholds corresponding to the levels in Table 2 (see first column of Table 3). Cumulative counts out of 364 counts listed in the last two columns are based on the time history of bar charts of numbers of sectors in peak climb-count levels like the one shown in Fig. 5. Cumulative counts were discussed earlier to explain the contents of Table 3. The value of 364 in the sixth and seventh columns indicates that at no time were there more than 14 aircraft in climb in a higher altitude sector.

Table 6. Numbers of sectors with peak cruise-counts using actual track-data.

Level	Min.	Mean	Max.	Threshold	Cumulative Lower	Cumulative Upper
1	19	136	340	5	19	340
2	24	140	220	10	175	364
3	0	70	149	15	324	364
4	0	15	36	20	355	364
5	0	2	6	25	361	364
6	0	0	3	30	363	364
7	0	0	0	35	363	364
8	0	0	1	42	364	364

Table 7. Numbers of sectors with peak descent-counts using actual track-data.

Level	Min.	Mean	Max.	Threshold	Cumulative Lower	Cumulative Upper
1	323	345	364	5	323	364
2	0	19	41	10	363	364
3	0	0	1	15	364	364

Table 8. Numbers of sectors with peak jet-counts using ACES data.

Level	Min.	Mean	Max.	Threshold	Cumulative Lower	Cumulative Upper
1	7	112	341	5	7	341
2	22	134	219	10	144	363
3	1	94	175	15	305	364
4	0	22	52	20	352	364
5	0	3	12	25	362	364
6	0	0	2	30	364	364

Table 9. Numbers of sectors with peak non-jet-counts using ACES data.

Level	Peak Non-jet Count	Min.	Mean	Max.	Threshold	Cumulative Lower	Cumulative Upper
1	0	202	278	361	1	202	361
2	1	3	66	117	2	306	364
3	2	0	16	43	3	349	364
4	3	0	4	15	4	358	364
5	4	0	1	6	5	362	364
6	5	0	0	2	6	364	364

Tables 6 through 10 should be interpreted in the same way as Table 5. Observe that the thresholds in Tables 9 and 10 are not the ones in Table 2. Since there are far fewer non-jet aircraft and conflicts compared to the number of aircraft in a sector, the thresholds for non-jet aircraft counts and conflict-counts have a smaller range compared to those in Table 2.

B. Separation Metrics

The next four metrics, eight through twelve in Table 4, are separation metrics described in Ref. 8. The first horizontal separation metric, C7 in Ref. 8, considers a vertical neighborhood of ± 2000 feet around each aircraft in the sector. Horizontal distance to the closest aircraft in the vertical neighborhood is then computed. These distances are added and the average minimum separation is computed. The second horizontal separation metric, C9 in Ref. 8, is the minimum horizontal separation obtained within the altitude bands. It is the minimum of the horizontal distances, rather than the average, computed in the previous metric.

Table 10. Numbers of sectors with peak conflict-counts using ACES data.

Level	Peak Conflict-Count	Min.	Mean	Max.	Threshold	Cumulative Lower	Cumulative Upper
1	0	36	142	347	1	36	347
2	1	17	154	232	2	224	364
3	2	0	45	90	3	314	364
4	3	0	17	41	4	347	364
5	4	0	4	12	5	359	364
6	5	0	1	4	6	362	364
7	6	0	0	2	7	363	364
8	7	0	0	1	8	364	364

The two vertical separation metrics are computed in a similar manner as the horizontal separation metrics. The first vertical separation metric, C8 in Ref. 8, places a horizontal neighborhood of ten nautical-miles around each aircraft in the sector. Vertical separation distance to the closest aircraft in the horizontal neighborhood is computed. The distances are then summed up to determine the average vertical separation. The second metric, C10 in Ref. 8, is the minimum of these vertical separation distances.

The time to conflict is computed as the ratio of the range to the range-rate (time derivative of range). The average time-to-go, defined as C12 in Ref. 8, considers each aircraft in the sector one at a time for determining the aircraft with which it is predicted to conflict. Next, the time-to-go is used for identifying those aircraft (conflict set) with which conflict is predicted in the near term (for example, in less than ten minutes). Minimum time-to-go is then determined for each conflict set, summed and divided by the number of sets to compute the average.

Minimum values of the 1) two horizontal separation metrics, 2) two vertical separation metrics, and 3) one time-to-go metric were computed for each hour using actual track-data. Time histories and historgrams of sectors were created in the same manner as discussed for the traffic-count metrics. The trends in these data are summarized in Tables 11 through 15.

Table 11. Numbers of sectors with minimum average-minimum-horizontal-separation (nautical-miles) using actual track-data.

Level	Min. Separation Range	Min.	Mean	Max.	Threshold	Cumulative Lower	Cumulative Upper
1	0-4	76	122	160	5	76	160
2	5-9	15	60	95	10	93	214
3	9-165	60	141	191	166	262	364
4	No-conflict	0	41	202	≥ 0	364	364

Table 12. Numbers of sectors with minimum minimum-horizontal-separation (nautical-miles) using actual track-data.

Level	Min. Separation Range	Min.	Mean	Max.	Threshold	Cumulative Lower	Cumulative Upper
1	0-4	93	268	344	5	93	344
2	5-9	14	22	34	10	110	361
3	9-165	2	33	90	166	162	364
4	No-conflict	0	41	202	≥ 0	364	364

The category *no-conflict* in Tables 11 and 12 means that aircraft in the sector were outside each others vertical bounds, therefore horizontal separation was not computed for them. Horizontal separation is measured in nautical-miles and the vertical separation is measured in feet. Time-to-go is measured in seconds. The categories *no-conflict* in Tables 13 and 14 means that aircraft were outside each others horizontal bounds, and 'at most one aircraft' in

Table 15 means that there were sectors that had just one aircraft or none, therefore time-to-go was not computed for them.

Table 13. Numbers of sectors with minimum average-minimum-vertical-separation (feet) using actual track-data.

Level	Min. Separation Range	Min.	Mean	Max.	Threshold	Cumulative Lower	Cumulative Upper
1	0-999	104	281	353	1000	104	353
2	1000-9700	11	22	43	9701	122	364
3	No-conflict	0	60	242	≥ 0	364	364

Table 14. Numbers of sectors with minimum minimum-vertical-separation (feet) using actual track-data.

Level	Min. Separation Range	Min.	Mean	Max.	Threshold	Cumulative Lower	Cumulative Upper
1	0-999	105	287	359	1000	105	359
2	1000-9700	5	16	34	9701	122	364
3	No-conflict	0	60	242	≥ 0	364	364

Table 15. Numbers of sectors with minimum average-minimum-time-to-go (seconds) using actual track-data.

Level	Min. Time-to-go Range	Min.	Mean	Max.	Threshold	Cumulative Lower	Cumulative Upper
1	0-119	13	126	211	120	13	211
2	120-239	15	94	144	240	34	336
3	240-359	8	26	58	360	42	357
4	360-479	1	11	24	480	48	358
5	480-599	1	7	24	600	59	361
6	At most one aircraft	3	99	305	≥ 0	364	364

C. Flow Metrics

The three flow metrics discussed in this section are, average transit-time, average airspeed and the variance in airspeed of aircraft in the sector.

Sector transit-time is defined as the time taken by the aircraft to cross the sector. The difference between the entry and exit times, obtained by processing the actual track-data provided the transit-time. Average transit-time for each sector was obtained by considering the transit-time of all the aircraft that went though the sector during the 24-hour period. Figure 6 shows the histogram of the average transit-time in minutes of 364 higher altitude sectors. The minimum, mean, standard-deviation, and maximum values of the distribution shown in Fig. 6 were found to be 2.8 minutes, 8 minutes, 2.8 minutes and 21 minutes.

Average airspeed was computed every ten-second in each sector using the ACES simulated data. Maximum average-airspeed within each hour was computed with 360 such values. Time histories and bar charts of sectors were then created with the maximum average-airspeed values. Results are summarized in Fig. 7 and Table 16. Observe that airspeed of higher altitude traffic generally lies in the 400 knots to 500 knots range.

Like the average airspeed, the variance of airspeed (knots^2) was computed at ten-second intervals and then the maximum value was selected for each hour for each sector. Variance of airspeed is defined in Eq. 26 in Ref. 8. Time history of the bar charts of sectors with the maximum airspeed-variance in six-levels is shown in Fig. 8. Table 17 lists the five-levels, minimum, maximum, average, and maximum number of sectors at each of the five-levels, and the cumulative lower and upper bounds obtained using the bar charts in Fig. 8.

The computations done with airspeed could have also been done with groundspeed, which is available in the actual track-data, but it was not used because groundspeed depends on winds, which vary from day to day. Airspeed on the other hand is a function of aircraft performance characteristics and is independent of winds.

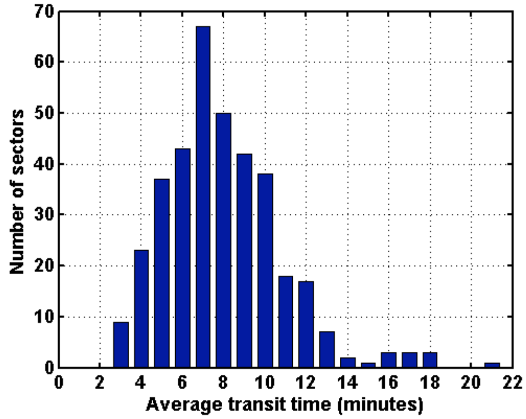

Figure 6. Histogram of average transit-time of 364 high-altitude sectors.

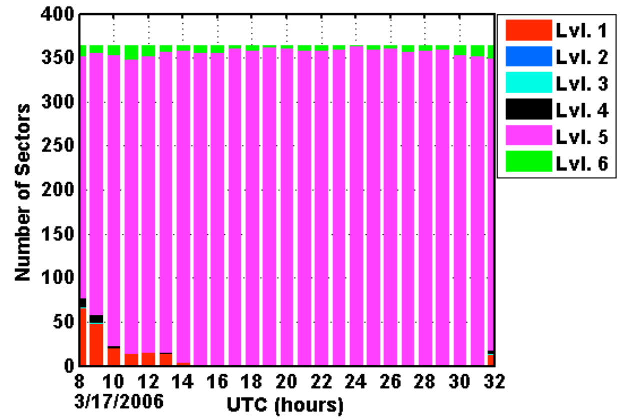

Figure 7. Time-history of histograms of number of sectors grouped in six peak average-airspeed levels in Table 16 using ACES data.

Table 16. Numbers of sectors with maximum average-airspeed (knots) using ACES data.

Level	Max. Average-Airpeed Range	Min.	Mean	Max.	Threshold	Cumulative Lower	Cumulative Upper
1	0-99	0	8	66	100	0	66
2	100-199	0	0	0	200	0	66
3	200-299	0	0	2	300	0	68
4	300-399	0	1	9	400	0	77
5	400-499	276	348	364	500	349	364
6	500-524	0	7	15	525	364	364

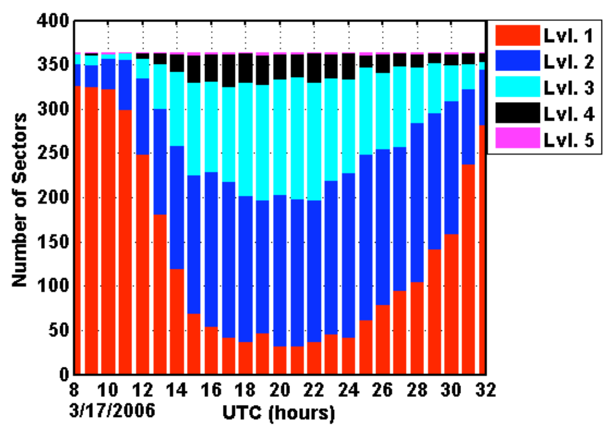

Figure 8. Time-history of histograms of number of sectors grouped in five peak airspeed-variance levels in Table 17 using ACES data.

Table 17. Numbers of sectors with maximum airspeed-variance (knots^2) using ACES data.

Level	Max. Airspeed-variance Range	Min.	Mean	Max.	Threshold	Cumulative Lower	Cumulative Upper
1	0-29	33	137	327	30	33	327
2	30-59	25	133	187	60	197	358
3	60-89	5	74	138	90	326	364
4	90-119	0	18	37	120	361	364
5	120-140	0	1	3	141	364	364

IV. Geometric Metrics

Geometric metrics are described in this section. Sector geometry features such as airways, navigational aids and airports define the kind and the frequency of tasks performed by the controller. Therefore, they contribute to controller workload directly and operational errors indirectly.[10,11] Sector geometry metrics, including those proposed in Refs. 10 and 11, considered in this study are listed in Table 18. Data resulting from computations on higher altitude sectors are discussed in the subsections below.

Geometric metrics listed in Table 18 are grouped into five categories. The first category "Geographical Location" consists of metrics one through three. The second category "Sector Dimensions" consists of metrics four through seven. The third category "Shape Attributes" consists of metrics eight through ten. The fourth category "Route Attributes" comprises of metrics 11 through 15. The last category "Neighborhood Attributes" contains metrics 16 through 18.

Table 18. Sector geometry metrics.

Number	Metric	Category
1	Number of sectors in centers	Geographical
2	Number of sectors in eight air traffic control regions	Geographical
3	Sector-type: low, high or super-high	Geographical
4	Sector volume	Dimensions
5	Sector height	Dimensions
6	Sector area	Dimensions
7	Sector length	Dimensions
8	Aspect ratio – length/width	Shape
9	Principal direction	Shape
10	Number of subsectors	Shape
11	Number of navaids	Route
12	Number of intersections	Route
13	Number of airways	Route
14	Number of airports	Route
15	Special Use Airspace completely inside	Route
16	Number of surrounding sectors	Neighborhood
17	Special Use Airspace contained partially	Neighborhood
18	Distance to closest major airport	Neighborhood

A. Geographical Location

The number of higher altitude sectors in each center was determined from the first three characters of Sector IDs of sectors with a base of 17,100 feet and above. For example, "ZAB37" indicates that the sector belongs to the Albuquerque center (ZAB). Counting all these sectors shown in Fig. 1 with the same first three letters provided the number of sectors in each center shown in Table 19.

Table 19. Numbers of sectors in centers.

Center ID	ZAB	ZAU	ZBW	ZDC	ZDV	ZFW	ZHU	ZID	ZJX	ZKC
# sectors	23	25	13	19	28	18	17	25	20	27
Center ID	ZLA	ZLC	ZMA	ZME	ZMP	ZNY	ZOA	ZOB	ZSE	ZTL
# sectors	16	8	6	21	18	10	11	27	10	22

The 20 centers listed in Table 19 are organized in eight geographical regions listed in Table 20. The number of sectors in each region is obtained by summing the values corresponding to the centers that form the region. These results are given in the fourth column of Table 20.

Table 20. Centers in eight regions.

Regions	Code	Centers	# sectors
Central Region	ACE	ZKC	27
Eastern Region	AEA	ZNY, ZDC	29
Great Lakes Region	AGL	ZMP, ZAU, ZID, ZOB	95
New England Region	ANE	ZBW	13
Northwest Mountain Region	ANM	ZSE, ZLC, ZDV	46
Southern Region	ASO	ZME, ZTL, ZJX, ZMA	69
Southwest Region	ASW	ZAB, ZFW, ZHU	58
Western Pacific Region	AWP	ZOA, ZLA	27

The numbers of low-altitude, high-altitude and super-high-altitude sectors as defined in May 2007 ETMS adaptation data were found to be five, 248 and 111, respectively. The five low-altitude sectors had a base at or above 17,100 feet altitude.

B. Sector Dimensions

To determine the dimensions of each sector, the volume of each subsector was computed. A subsector is defined as a polygonal prism with a boundary defined by a polygon and a constant height. The complex geometric shape of a sector is achieved by placing subsectors on top, and to the side of other subsectors. The volume of a sector is the sum of the volumes of its subsectors. Figure 9 shows the histogram of the volume of sectors, in cubic-nautical-miles.

Height of each sector was determined by subtracting the lower bound of the lowest subsector from the upper bound of the highest subsector. The distribution of the heights of the sectors is shown in Fig. 10. The histogram in Fig. 10 shows a bi-modal distribution with sector heights below 16,000 feet and above 56,000 feet.

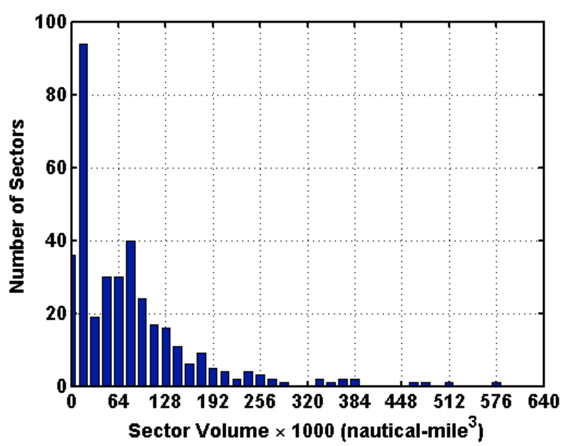

Figure 9. Sector volume histogram.

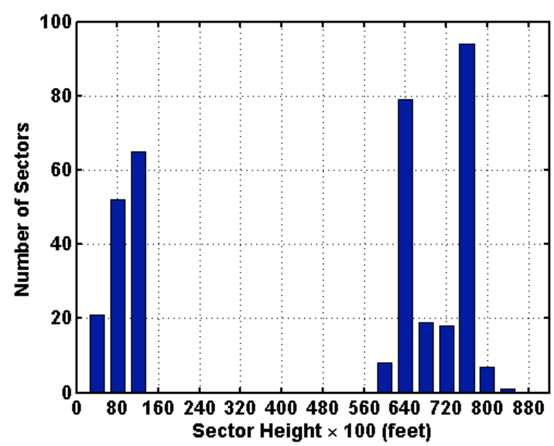

Figure 10. Sector height histogram.

Dividing sector volumes with sector heights resulted in the reference-areas of the sectors. The distribution of the sector reference-areas is shown in Fig. 11. Reference-lengths of the sectors were obtained by taking the square-root of the reference-areas. The histogram of the reference-lengths is given in Fig. 12.

Minimum, mean, maximum and standard deviation values of sector volume, height, reference-area and reference-length are summarized in Table 21.

C. Shape Attributes

Aspect-ratio, the ratio of the length to width, of the sectors was determined by computing the moments of inertia of the sectors. Prior to the computation of moments of inertia, centroids of the sectors had to be computed. Since a sector is composed of subsectors, the centroid of each subsector was determined first, and then, these centroids were weighted with the volumes of the subsectors to obtain the centroid of the sector. The moment of inertia tensor of

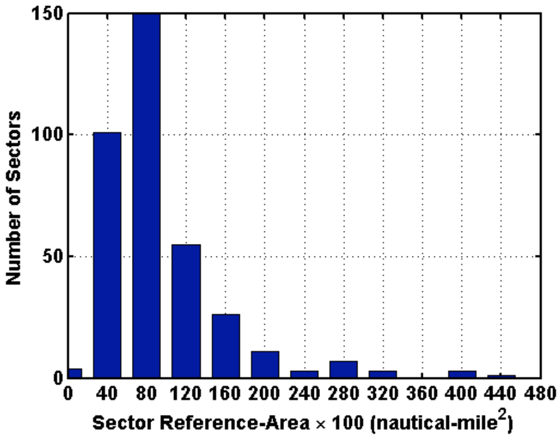

Figure 11. Sector reference-area histogram.

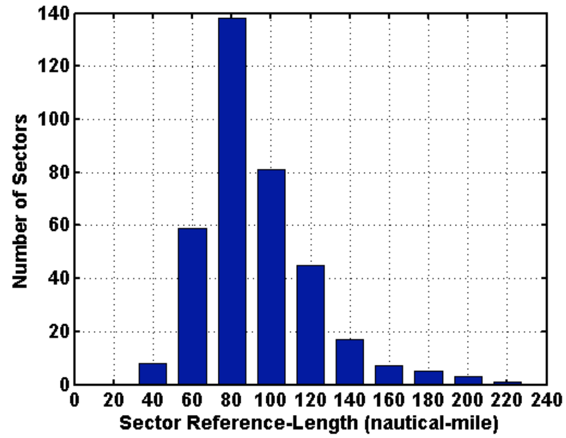

Figure 12. Sector reference-length histogram.

Table 21. Summary of sector dimensions.

Metric	Minimum	Mean	Maximum	Std. Dev.
Volume (cubic-nautical-mile)	1,909	77,775	572, 210	86,034
Height (feet)	4,000	47,541	82,850	30,164
Area (square-nautical-mile)	1,678	9,397	45,778	6,369
Length (nautical-mile)	41	93	214	28

each subsector was computed with respect to the frame of reference located at the centroids, and then the parallel axis theorem was employed to determine the moment of inertia tensor with respect to the frame of reference located at the centroid of the sector. These moment of inertia tensors were then summed up to determine the moment of inertia tensor of the sector. Mathematical expressions for computing the centroid and the moment of inertia tensor for a two-dimensional polygonal object are given in Ref. 20. These equations were extended to three-dimensional polygonal prisms for generating the results discussed here.

The eigenvalues of the moment of inertia tensor are the principal moments of inertia about the principal axes, which are the eigenvectors corresponding to the eigenvalues. If I_{11}, I_{22} and I_{33} are the principal moments of inertia, the dimensions of a rectangular prism with the same principal moments of inertia as the sector (polygonal prism) are:

$$l_i = \sqrt{\frac{12}{V}\left(S - I_{ii}\right)}; \quad 1 \le i \le 3 \tag{1}$$

where,

$$S = \frac{1}{2}\left(I_{11} + I_{22} + I_{33}\right)$$

and V is the volume of the sector. The aspect-ratio is given by the ratio of dimensions in Eq. (1), l_i / l_j such that $i \neq j$.

Figure 13 shows the distribution of the aspect-ratio of the 364 sectors. Sectors with an aspect-ratio close to one are of square shape, while the sector with an aspect-ratio closer to seven is a highly elongated rectangle. The minimum, mean, maximum and standard deviation aspect-ratio are 1.0, 2.0, 6.6, and 0.86, respectively. Reference 7 notes that the traffic pattern is usually highly parallel and less complicated in elongated sectors.

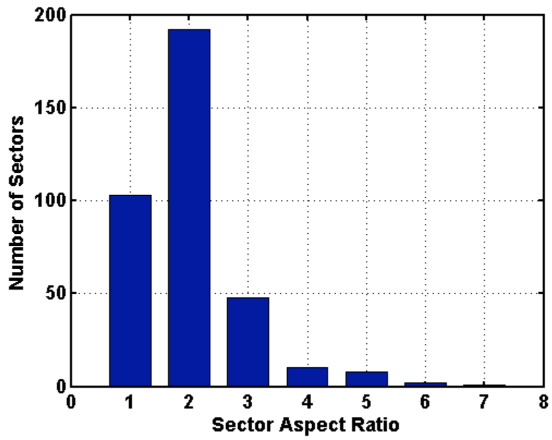

Figure 13. Sector aspect-ratio histogram.

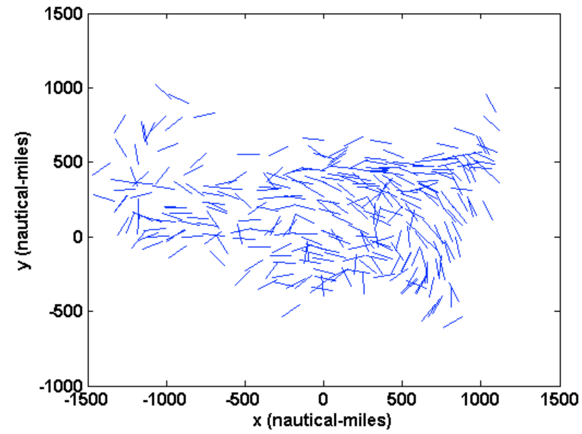

Figure 14. Preferred axis of the sectors.

If the principal moments of inertia are distinct, the principal axes are uniquely specified. If two or all three of the principal moments are the same, there is no choice of a preferred axis.

Once the three principal axes were obtained, the two principal axes with larger projections on the horizontal plane were selected. Of these, the one with the larger eigenvalue was chosen as the preferred axis of the sector. Figure 14 shows the preferred axis of the sectors. This figure shows that most of the sectors are aligned along East-West direction. Along the East and West Coasts, sectors are oriented in the North-South direction. It is interesting that the sectors are aligned along the major traffic flow directions.

The number of subsectors in a sector is an indicator of the shape complexity of the sector. Table 22 lists the number of sectors containing the same number of subsectors. This table shows that most of the sectors have a single subsector. One sector has 13 subsectors. The mean and the standard deviation of the number of subsectors were found to be 1.7 and 1.4.

Table 22. Numbers of subsectors in sectors.

# Subsectors	# Sectors
1	224
2	97
3	22
4	6
5	5
6	3
7	1
8	3
9	1
12	1
13	1

D. Route Attributes

Three types of navigation aids were counted to determine the number of navigation aids in sectors. These three types of radio navigation aids commonly employed by aircraft for navigation along routes are Very-High-Frequency Omnidirectional Range (VOR), VOR collocated with Distance Measuring Equipment (VOR-DME), and VOR collocated with Tactical Air Navigation System (VORTAC). The known latitude and longitude of each navigation aid were used for locating it in the sector. Figure 15 shows the distribution of sectors as a function of the number of navigation aids enclosed within their boundaries. There are a total of 1055 navigation aids. Some of these are shared by multiple sectors. Six sectors had no navigation aids and one sector had a maximum of 14 navigation aids. The mean and standard deviation of the number of navaids in a sector is 3.9 and 2.3.

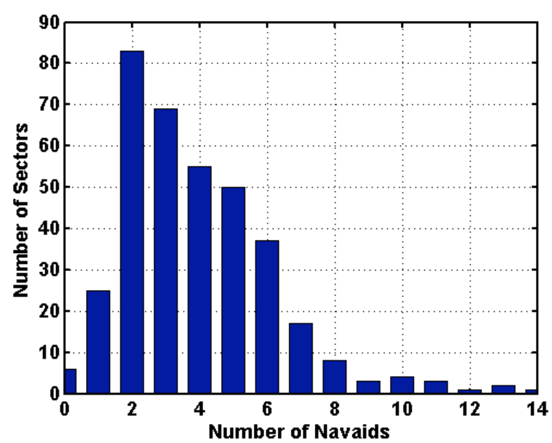

Figure 15. Sector navigation aids histogram.

Next, the number of intersections in sectors was computed. Intersections are defined as locations where airways, Victor Airways and Jet Routes, intersect. Intersections are specified by latitude, longitude and altitude. This makes it possible to locate them in sectors. Figure 16 shows the histogram of sectors based on the number of intersections enclosed within the sectors. Sixty-four sectors had no intersections, 328 sectors had ten or fewer intersections, 36 sectors had more than 10 intersections, and one sector had 22 intersections. Mean and standard deviation were determined to be 4.3 and 4.1 intersections.

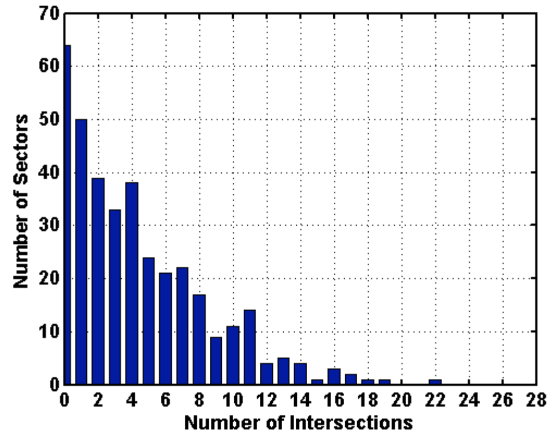

Figure 16. Sector intersections histogram.

Airways in sectors were determined using the association between the intersections and airways. Since an airway can be associated with several intersections within a sector, each associated airway is counted only once. An airway that went across the sector without passing through an intersection in the sector could not be counted. It may be possible to improve the airway count by using the association between the navaids and airways in addition to that between intersections and airways. Victor Airways were counted below 18,000 feet altitude and Jet Routes at or above 18,000 feet altitude. Both were counted in sectors whose base was below 18,000 feet and top above 18,000 feet altitude. A histogram of sectors as a function of the number of airways is given in Fig. 17. Airways were not found in sixty-four sectors because those sectors did not have any intersections. 334 sectors had ten or fewer airways while 30 sectors had more than ten airways. The maximum number of airways was found to be 17 in only one sector. Mean and standard deviation values were determined to be 5 and 3.7 airways.

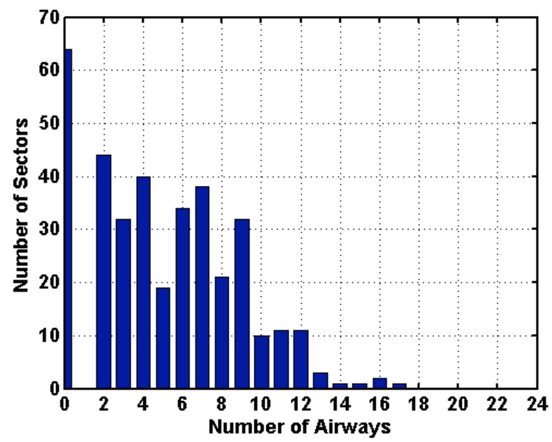

Figure 17. Sector airways histogram.

Seventy-four major airports in the United States that are in the Federal Aviation Administration's (FAA) Aviation System Performance Metrics (ASPM)[21] were located within the horizontal confines of the higher altitude sectors and counted. Table 23 lists the numbers of sectors and the corresponding numbers of 74 ASPM airports. Eighty-three sectors had one or more major U. S. airports. Only 16 sectors had two or more airports.

Table 23. Numbers of 74 ASPM airports in sectors.

# Airports	# Sectors
0	281
1	67
2	10
3	5
5	1

Controllers have to ensure that aircraft do not enter a Special Use Airspace (SUA). This monitoring function adds to controller workload. Prohibited areas, military operations areas, alert areas, warning areas, and national security areas are considered to be SUA. Boundary and height information of the 1017 SUAs obtained from the FAA were used for locating them in sectors. Of the 364 sectors, only two sectors, ZHU 59 and ZDV 47 were found to completely contain one and two SUAs, respectively. The rest partially contained the SUAs. Statistics of sectors partially containing SUAs are discussed in the next subsection.

E. Neighborhood Attributes

Sectors above, below and to the sides of sectors were counted to determine the number of surrounding sectors. Minimum, mean, maximum and standard deviation of the number of surrounding sectors were determined to be 4, 13.3, 30 and 3.9. Sector 22 in Atlanta Center was found to have 30 sectors surrounding it. There were 202 sectors that had 13 or fewer sectors surrounding them, while 162 sectors had more than 13 sectors surrounding them.

The distribution of the sectors as a function of number of surrounding sectors is given in Fig. 18.

SUA polygons were related to a data structure of grid cells using the method described in Ref. 14. The mapping of the grid cells to the sectors was then used to identify the set of sectors that the SUAs could be in. The altitude range of the sectors was compared with the altitude range of the SUAs to determine if there was any overlap. Sectors with overlap were deemed to partially or fully contain these SUAs. If a SUA was associated with a single sector, that sector was considered to completely contain that SUA. In instances where the SUA was associated with more than one sector, the SUA was considered to be partially contained in the associated sectors. With the elimination of two sectors that fully contained SUAs, analysis was done on the remaining 362 sectors. SUAs were not found in 268 sectors. Eighty-one sectors were found to have five or fewer SUAs. Only 15 sectors were found to have more than five SUAs. Sector 26 in Houston Center contained 19 SUAs. Table 24 summarizes these results.

Distance with respect to the center of the sector to the closest one of the 74 ASPM airports outside the sector was determined by first establishing which of them were within the confines of the sector boundary. These airports were excluded and distances to the airports outside the sector boundary were computed. The minimum of these distances gave the distance to the closest airport outside the sector. Figure 19 gives the histogram of the sectors with respect to distances to the closest airports. The closest airport outside a sector was 20.6 nautical-miles. The average and maximum distances were 116.5 and 422.2 nautical-miles. The standard deviation was 57.8 nautical-miles. A major airport was within 200 nautical-miles from the 335 sectors (both inside and outside the sector). Only 29 sectors were farther than 200 nautical-miles from a major airport.

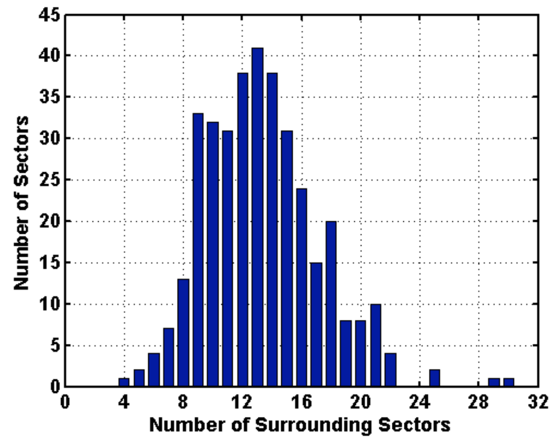

Figure 18. Surrounding sectors histogram.

Table 24. Number of SUAs contained partially in sectors.

# SUAs	# Sectors	# SUAs	# Sectors
0	268	7	1
1	31	8	2
2	22	9	1
3	12	10	1
4	8	11	1
5	8	12	3
6	3	19	1

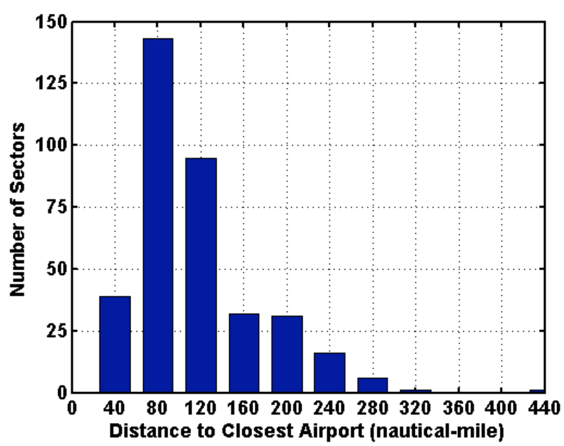

Figure 19. Distance to closest airport outside the sector histogram.

V. Summary

This paper was motivated by the problem of determining the design features of the current sectors so that future designs can be compared with the current design. Since the current design is based on tools and techniques used by controllers, a large departure from this design guided by automation needs will have implications in controllers being able to manage traffic in the new sectors.

Since this study is focused on current sectors, fifteen traffic metrics related and eighteen geometric metrics related to controller workload were used to characterize the design of current sectors. Numerical values of these metrics were computed for sectors with a base of 17,100 feet and above in the current U. S. airspace. The fifteen traffic metrics were classified into three categories: seven traffic-count metrics, five separation metrics and three flow metrics. The eighteen geometric metrics were classified into five categories: three geographical location metrics, four sector dimension metrics, three shape attribute metrics, five route attribute metrics and three neighborhood attribute metrics. Ten out of the fifteen traffic metrics were computed using actual aircraft position data obtained from the field and the remaining five were computed using simulated aircraft position data. Use of simulated data provided an easy means of computing conflict-count, aircraft type and airspeed metrics. Conflict-counts are difficult to determine from actual data because controllers make sure that aircraft are separated. Only in rare occasions operational errors occur when separation minimums are violated. Aircraft type and airspeed information is available in the flight-plan therefore it is straightforward to carry this information in a simulation. It is possible to relate the flight-plan data to aircraft position update messages using aircraft identification tag that is common to both, but the processing is more involved. Maximum numbers of aircraft in sectors during the 24-hour period were computed using both actual and simulated data. Time histories were presented to show that the results obtained using simulated data compare very well with those obtained using actual data.

Data corresponding to the distribution of sectors as a function of the traffic and geometric metric values were provided in tables and in bar charts. These results show that most sectors in the current airspace have fewer than 20 aircraft at any given time. Most sectors have less than five aircraft in climb phase, fifteen in cruise phase and five in descent phase. Most of the traffic at higher altitude sectors is jet traffic. It was shown that about 98% of the sectors have fewer that three pairs of aircraft in conflict in simulation. Horizontal and vertical separation metrics indicated that aircraft fly at the same altitude in most sectors. Airspeed was found to lie in a narrow range of 400 to 500 knots. Sector transit time was found to be normally distributed with a mean of eight minutes and standard deviation of three minutes. The maximum transit time was found to be 21 minutes. A wide variation was found in sector volume, area, height and length. Most sectors were found to be elongated with an aspect ratio of two and aligned with the main traffic flows. The number of subsectors, which is a measure of sector shape complexity, was found to be less than three in most sectors. Of the 364 sectors considered in this study, 328 sectors had ten or fewer airway intersections. Maximum number of airways in a sector was determined to be 17. On an average, a sector was surrounded by 13 other sectors. The maximum number of sectors surrounding a sector was found to be 30. None of the 1017 Special Use Airspaces (SUAs) were found in 268 sectors. Eighty-one sectors had five or fewer SUAs. The maximum number of SUAs in a sector was determined to be 19. A major U. S. airport was found within 200 nautical-miles from each of the 335 sectors. Only 29 sectors were farther than 200 nautical-miles from one of the 74 major U. S. airports.

References

[1]Kopardekar, P., Bilimoria, K., and Sridhar, B., "Initial Concepts for Dynamic Airspace Configuration," *Proceedings of 7th AIAA Aviation Technology, Integration and Operations Conference (ATIO),* Belfast, Northern Ireland, September 18-20, 2007.

[2]Martinez, S., Chatterji, G. B., Sun, D., and Bayen, A., "A Weighted-Graph Approach for Dynamic Airspace Configuration," *Proceedings of AIAA Guidance, Navigation, and Control Conference,* Hilton Head, SC, August 20-23, 2007.

[3]Yousefi, A., and Donohue, G. L., "Temporal and Spatial Distribution of Airspace Complexity for Air Traffic Controller Workload-Based Sectorization," Proceedings of AIAA 4th Aviation Technology, Integration and Operations (ATIO) Forum, Chicago, IL, September 20-22, 2004.

[4]Pawlak, W. S., Goel, V., Rothenberg, D. B., and Brinton, C. R., "Comparison of Algorithms for the Dynamic Resectorization of Airspace," *Proceedings of AIAA Guidance, Navigation, and Control Conference,* Boston, MA, August 10-12, 1998.

[5]Christien, R., and Benkouar, A., "Air Traffic Complexity Indicators and ATC Sectors Classification," *Proceedings of 5th USA/Europe Air Traffic management R&D Seminar,* Budapest, Hungary, June 23-27, 2003.

[6]Basu A., Mitchell, J. S. B., and Sabhnani, G., "Geometric Algorithms for Optimal Design and Air Traffic Controller Workload Balancing," *16th Fall Workshop on Computational and Combinatorial Geometry,* Northampton, MA, November 10-11, 2006.

[7]Yousefi, A., Donohue, G. L., and Qureshi, K. M., "Investigation of En route Metrics for Model Validation and Airspace Design Using the Total Airport and Airspace Modeler (TAAM)," Proceedings of the *5th Eurocontrol/FAA ATM R&D Conference*, Budapest, Hungary, June 23-27, 2003.

[8]Chatterji, G. B., and Sridhar, B., "Measures for Air Traffic Controller Workload Prediction," *Proceedings of AIAA Aircraft, Technology, Integration, and Operations Forum*, Los Angeles, CA, October 16-18, 2001.

[9]Kopardekar, P., et al, "Airspace Complexity Measurement: An Air Traffic Control Simulation Analysis," *Proceedings of 7th USA/Europe ATM R&D Seminar*, Barcelona, Spain, July 2-5, 2007.

[10]Mogford, R. H., Murphy, E. D., and Guttman, J. A.,"Using Knowledge Exploration Tools to Study Airspace Complexity in Air Traffic Control," *International Journal of Aviation Psychology*, vol. 4, No. 1, January, 1994, pp. 29-45.

[11]Goldman, S., Manning, C., and Pfleiderer, E., "Static Sector Characteristics and Operational Errors," Report No. DOT/FAA/AM-06/4, Office of Aerospace Medicine, Federal Aviation Administration, 800 Independence Ave., S. W., Washington, DC 20591, March, 2006.

[12]Chatterji, G. B., Sridhar, S., Kim, D., "Analysis of ETMS Data Quality for Traffic Flow Management Decisions," AIAA-2003-5626, *Proceedings of AIAA Guidance, Navigation, and Control Conference,* Austin, TX, August 11-14, 2003.

[13]Volpe National Transportation Systems Center, "Aircraft Situation Display To Industry: Functional Description and Interface Control Document," Version 4.0, Report No. ASDI-FD-001, Volpe National Transportation Systems Center, Automation Applications Division, DTS-56, 55 Broadway Street, Cambridge, MA 02142, August 4, 2000.

[14]Sahlman, S., "Description and Analysis of a High Fidelity Airspace Model for the Airspace Concept Evaluation System," AIAA-2007-6877, *Proceedings of AIAA Modeling and Simulation Technologies Conference and Exhibit,* Hilton Head, SC, August 20-23, 2007.

[15]URL: http://www.mysql.com/[cited 14 July 2008].

[16]Meyn, L., et al, "Build 4 of the Airspace Concept Evaluation System," AIAA-2006-6110, *Proceedings of AIAA Modeling and Simulation Technologies Conference and Exhibit*, Keystone, Colorado, August 21-24, 2006.

[17]Zelinski, S. J., "Validating The Airspace Concept Evaluation System Using Real World Data," AIAA 2005-6491, *Proceedings of AIAA Modeling and Simulation Technologies Conference and Exhibit,* San Francisco, CA, August 15-18, 2005

[18]Zelinski, S. J., and Meyn, L., "Validating The Airspace Concept Evaluation System For Different Weather Days," AIAA 2006-6115, *Proceedings of AIAA Modeling and Simulation Technologies Conference and Exhibit,* Keystone, CO, August 21-24, 2006.

[19]Chatterji, G. B., and Zheng, Y., "Impact of Airport Capacity Constraints on National Airspace System Delays," AIAA-2007-7712, *Proceedings of 7th AIAA Aviation Technology, Integration and Operations Conference (ATIO),* Belfast, Northern Ireland, September 18-20, 2007.

[20]Lee, H., and Romer T. F., "Automating the Process of Terminal Area Node-Link Model Generation," *Proceedings of AIAA Modeling and Simulation Technologies Conference and Exhibit,* Honolulu, Hawaii, August 18-21, 2008**.**

[21]URL: http://aspm.faa.gov/aspm/entryASPM.asp [cited 14 July 2008]

Acknowledgements

The authors thank Dr. Hak-Tae Lee of University of California Santa Cruz for generalizing the moment of inertia equations from two-dimensional polygons to three-dimensional polygonal prisms and providing the *Java* program that was used for computing the principal directions and aspect ratio of sectors. We also thank Christopher Gleim from the University of Louisville who as a part of his internship task wrote the computer program for the Special Use Airspace analysis discussed in this paper.